Structure and magnetic properties of polydisperse ferrofluids: A molecular dynamics study

Zuowei Wang* and Christian Holm†
Max-Planck-Institut für Polymerforschung, Ackermannweg 10, D-55128 Mainz, Germany
(Received 5 June 2003; published 2 October 2003)

We study by Langevin molecular dynamics simulations systematically the influence of polydispersity in the particle size, and subsequently in the dipole moment, on the physical properties of ferrofluids. The polydispersity is in a first approximation modeled by a bidisperse system that consists of small and large particles at different ratios of their volume fractions. In the first part of our investigations the total volume fraction of the system is fixed, and the volume fraction ϕ_L of the large particles is varied. The initial susceptibility χ and magnetization curve of the systems show a strong dependence on the value of ϕ_L. With the increase of ϕ_L, the magnetization M of the system has a much faster increment at weak fields, and thus leads to a larger χ. We performed a cluster analysis that indicates that this is due to the aggregation of the large particles in the systems. The average size of these clusters increases with increasing ϕ_L. In the second part of our investigations, we fixed the volume fraction of the large particles, and increased the volume fraction ϕ_S of the small particles in order to study their influence on the chain formation of the large ones. We found that the average aggregate size formed by large particles decreases when ϕ_S is increased, demonstrating a significant effect of the small particles on the structural properties of the system. A topological analysis of the structure reveals that the majority of the small particles remain nonaggregated. Only a small number of them are attracted to the ends of the chains formed by large particles.

DOI: 10.1103/PhysRevE.68.041401 PACS number(s): 82.70.Dd, 61.20.Ja, 75.50.Mm, 82.20.Wt

I. INTRODUCTION

Ferrofluids (magnetic fluids) are colloidal suspensions containing single domain magnetic particles in a carrier liquid [1]. To prevent agglomeration of the particles, they are either electrostatically stabilized or coated by adding a stabilizing surfactant layer. As a result, the particles interact with each other by the long-range magnetic dipole-dipole potential as well as the electrostatic monopolar interactions or short-range symmetrical potentials. Experiments have revealed that various microstructures can be formed in ferrofluids due to these interactions [2–8], which strongly affect the macroscopic properties of the systems, and thus lead to many potential applications.

A number of theoretical and simulational works have contributed to the understanding of the structural properties of ferrofluids. Interesting topics include the occurrence of the ferroelectric phase or spontaneous magnetization [9–16], the chain formation [13,17–23], and the gas-liquid phase transition behavior [21,24–31]. However, a comparison of these results with experimental data is not straightforward since some aspects of real systems are still not thoroughly taken into account by the simplified models. One example is the description of the steric interactions between the particles. The phase diagram of the model systems is found to depend substantially on the employed short-range potentials [24–31]. Whether a minimum amount of dispersive energy, i.e., the attractive van der Waals energy, is needed to obtain a phase separation, which has been repeatedly observed in experiments of real ferrofluids [2–5], is still one of the questions under debate.

Another important aspect deals with the polydispersity of the fluid. Most of the above mentioned theoretical and simulational works are based on a monodisperse model fluid. However, the particles in real ferrofluids always have a log-normal or γ size distribution, with a mean magnetic core diameter of about 10 nm [8,32,33]. Since the dipole moments of the particles are proportional to the volume of their magnetic cores, the larger particles can be oriented more easily at low field strengths, and the smaller ones can only be oriented under rather strong applied magnetic fields. As a result, the magnetization properties of a polydisperse system differ from that of a monodisperse system even in the very dilute case [8,34–37]. More importantly, a small fraction of large particles in the real system has a typical size of 15–20 nm. Since their dipole-dipole interaction energy is considerably larger than the thermal energy at room temperature, these particles can aggregate into different structures. Experiments have demonstrated that this small fraction of large particles can play a major role in determining the physical properties of polydisperse ferrofluids [5–8,38]. Their aggregation apparently enhances the effective viscosity at small flow velocity gradient [6–8,39] and the magnetization at weak fields [40] of various ferrofluid systems.

The structure of polydisperse ferrofluids was discussed theoretically on the basis of a bidisperse model where the systems are supposed to consist of two fractions of magnetic particles with significant size differences [39,41,42]. The main structural character in these systems is proposed to be the chainlike aggregates formed by the large particles. Some small particles might be attached to the ends of these aggregates, but most of them remain in the nonaggregated state [41,42]. This picture is consistent with the two-dimensional Monte Carlo (MC) simulation of a polydisperse system containing cobalt particles of small average diameter [40]. A phase separation has also been predicted for the bidisperse

*Electronic address: wangzuo@mpip-mainz.mpg.de
†Electronic address: holm@mpip-mainz.mpg.de

ferrofluid systems [43]. At least for a binary mixture of hard spheres with same dipole moments, but different diameters, the MC simulations did not reveal such a phase separation [44]. Instead, the formation of chains was observed when the diameter ratio of the particles is significantly different from 1. The Gibbs ensemble MC simulations have shown the demixing of a binary mixture of dipolar and neutral hard spheres of different sizes [45], in agreement with the prediction of an integral equation theory [46]. But this demixing is not observed in another MC simulation [44] of a similar binary system. This contradiction may be related to the range of the ratio of particle diameters where the neutral species can reduce the formation of dipolar chains or clusters that inhibit condensation of the pure dipolar hard-sphere fluids.

In this paper we employ Langevin molecular dynamics simulations to investigate the equilibrium properties of a bidisperse ferrofluid. The dependence of the magnetic properties and the aggregation behavior on the fractions of small and large particles are studied systematically for two cases. In the first investigated case the total volume fraction ϕ is fixed, and the volume fraction ϕ_L of the large particles is varied systematically. In the second case ϕ_L is fixed, and the volume fraction ϕ_S of the small particles is varied. The influence of the cluster formation on the magnetization curve and initial susceptibility of the systems are also discussed. The paper is organized as follows. We describe the simulation method in Sec. II. The simulation results are given and discussed in Sec. III. We end with our conclusions in Sec. IV.

II. SIMULATION METHOD

The ferrofluid systems investigated by us consist of N spherical particles distributed in a cubic simulation box of side length L. Each particle has a diameter of σ_i and a permanent point dipole moment $\mathbf{m_i}$ at its center. The dipole-dipole interaction potential between particles i and j is given by

$$U_{ij}^{dip}=\frac{1}{4\pi\mu_0}\left\{\frac{\mathbf{m}_i\cdot\mathbf{m}_j}{r_{ij}^3}-\frac{3(\mathbf{m}_i\cdot\mathbf{r}_{ij})(\mathbf{m}_j\cdot\mathbf{r}_{ij})}{r_{ij}^5}\right\}, \tag{1}$$

where $\mathbf{r}_{ij}=\mathbf{r}_i-\mathbf{r}_j$ is the displacement vector of the two particles and $\mu_0=4\pi\times10^{-7}$ H/m is the vacuum permeability. Using periodic boundary conditions in all spatial directions, the dipole-dipole interaction is evaluated by the Ewald summation under metallic boundary condition, which gives [47,48]

$$U_{ij}^{dip}=-(\mathbf{m}_i\cdot\boldsymbol{\nabla})(\mathbf{m}_j\cdot\boldsymbol{\nabla})\Psi(\mathbf{r}_{ij}) \tag{2}$$

with

$$\Psi(\mathbf{r})=\frac{1}{4\pi\mu_0}\left[\sum_{\mathbf{n}\in\mathbb{Z}^3}\frac{\mathrm{erfc}(\kappa|\mathbf{r}+\mathbf{n}L|)}{|\mathbf{r}+\mathbf{n}L|}+\frac{1}{\pi L}\sum_{n\neq0}n^{-2}\exp\left(\frac{-\pi^2n^2}{\kappa^2L^2}+\frac{2\pi i}{L}\mathbf{n}\cdot\mathbf{r}\right)\right]. \tag{3}$$

Here the sum in Eq. (3) is summed up in a spherical fashion and extends over all simple cubic lattice points $\mathbf{n}=(k,l,m)$ with k,l,m integers, and $\mathrm{erfc}(x)$ denotes the complementary error function. The inverse length κ is the splitting parameter of the Ewald sum which weights the relative contribution of the real and Fourier space parts. The use of the metallic boundary condition means that the demagnetization effects do not occur and the applied external magnetic field coincides exactly with the internal field [47–50]. The boundary condition effects in using Ewald summation in the simulation study of magnetic dipolar fluids had been discussed in Ref. [50]. The related formulas for the dipolar force $\mathbf{F}_{ij}^{dip}$ and torque $\boldsymbol{\tau}_{ij}^{dip}$ can be found in our previous paper [49], where we also derived theoretical estimates of the cutoff errors in the Ewald summation which are used to determine the optimal values for the Ewald parameters. This enabled us to minimize the overall computational time at a predefined accuracy.

The short-range interactions between the particles are represented by a purely repulsive Lennard-Jones potential. Considering the different sizes of the particles, this potential is written as

$$U_{ij}^{LJ}=4\varepsilon\left[\left(\frac{\sigma_i+\sigma_j}{2r_{ij}}\right)^{12}-\left(\frac{\sigma_i+\sigma_j}{2r_{ij}}\right)^{6}\right]+\varepsilon, \tag{4}$$

with a cutoff radius of $R_c=2^{-5/6}(\sigma_i+\sigma_j)$. In this way the particles have a purely repulsive force which smoothly decays to zero at R_c. Our molecular dynamics simulation method is similar to the Langevin dynamics implementation described in a previous work [23]. For simulating polydisperse systems, the variables can be defined according to a reference particle with diameter σ_0 which is normally taken as the mean size of the particles. In our bidisperse case, we take σ_0 to be the diameter of the small particles. In the following we are using reduced variables in dimensionless form such as length $r^*=r/\sigma_0$, dipole moment $m^{*2}=m^2/4\pi\mu_0\epsilon\sigma_0^3$, moment of inertia $I^*=I/(m_{a0}\sigma_0^2)$ with m_{a0} being the mass of the reference particle, time $t^*=t(\epsilon/m_{a0}\sigma_0^2)^{1/2}$, the friction constants $\Gamma_T^*=\Gamma_T(\sigma_0^2/m_{a0}\epsilon)^{1/2}$ and $\Gamma_R^*=\Gamma_R/(m_{a0}\sigma_0^2\epsilon)^{1/2}$, magnetic field $H^*=H(4\pi\mu_0\sigma_0^3/\epsilon)^{1/2}$, as well as temperature $T^*=kT/\epsilon$. Accordingly, the dimensionless translational and rotational equations of motion of particle i are given by

$$\sigma_i^{*3}\dot{\mathbf{v}}_i^*=\sum_{j\neq i}(\mathbf{F}_{ij}^{dip*}+\mathbf{F}_{ij}^{LJ*})-\Gamma_T^*\sigma_i^*\mathbf{v}_i^*+\boldsymbol{\xi}_i^{T*}, \tag{5}$$

$$\sigma_i^{*5}\mathbf{I}^*\cdot\dot{\boldsymbol{\omega}}_i^*=\sum_{j\neq i}\boldsymbol{\tau}_{ij}^{dip*}+\mathbf{m}_i^*\times\mathbf{H}^*-\Gamma_R^*\sigma_i^{*3}\boldsymbol{\omega}_i^*+\boldsymbol{\xi}_i^{R*}, \tag{6}$$

where $\boldsymbol{\xi}_i^{T*}$ and $\boldsymbol{\xi}_i^{R*}$ are the Gaussian random force and torque, respectively. The linear and cubic dependences of Γ_{Ti} and Γ_{Ri} on σ_i follow the concept of the first-order Stokes' frictions on the particles. In doing equilibrium simulations, the values of these friction constants employed are somewhat arbitrary. Here we adopted $\Gamma_T^*=10.0$ and $\Gamma_R^*=3.0$, because

these values had been found to speed up the equilibration time [23] and are close to that used in other Brownian dynamics simulations [51].

The simulations were performed at constant temperature $T^*=1$. An absolute root mean square error in the dipolar forces of $\Delta F^{dip} \leqslant 10^{-4} m_0^2/4\pi\mu_0\sigma_0^4$ was employed as the accuracy of the Ewald summation. A reduced time step of $\Delta t^*=2\sim 3\times 10^{-3}$ was used in the simulations. The runs were started from initial configurations with random particle positions and dipole moment orientations. The temporal evolution of the physical quantities that characterize the magnetization and structure properties of the systems were calculated during the simulations. These values were found to reach their stable states after a certain simulation time. Since no spontaneous magnetization occurs in these systems, the time for the structure properties (i.e., the average size of the clusters formed by particles) to reach their stable values was taken to be the characteristic time of setting up equilibrium state in the systems at zero field. When the external field is applied, the time for the magnetization to reach its stable value is, in general, longer than that of the structure properties, especially in case of weak fields and high fraction of large particles. In these cases the characteristic equilibration time is determined by the magnetization behavior of the systems. This equilibration time is about $t^*=100$ for the monodisperse system of small particles, but it could be as long as $t^*=500$ or more for the systems with high fraction of large particles. The total simulation time is at least three to four times longer than the equilibration time so as to make sure that the real stable states are reached. Since different friction constants could be chosen in order to speed up the equilibration, the simulation time for setting up the equilibrium state is not directly comparable with experiments. However, this does not affect the final results on the equilibrium properties [23,51]. The equilibrium values of the magnetization and structural properties were calculated for another period of at least $t^*=500$ after equilibration. Error bars for the simulation results were determined by dividing the simulation runs into blocks and calculating an estimate for the standard deviation of the mean [52,50]. In order to detect the influence of the initial state on the final results, we had generated and simulated several different random initial configurations for different cases. Starting from these different initial states, the calculated physical quantities evolve with time in similar routine and reach the stable states at similar simulation time. It confirms that our simulation results are obtained from the true equilibrium states of the systems. The final results show no significant dependence on the details of the initial configurations. They agree with each other within small error bars as will be seen below.

III. RESULTS AND DISCUSSIONS

Our bidisperse ferrofluid system consists of two fractions of magnetite particles with significantly different diameters. Following the experimental and theoretical discussions [8,39,41–43], a reasonable choice for the diameter of the small particles is the mean size of the real ferrofluid distribution. So σ_0 is taken to be 10 nm in our simulations. The diameter of the large particles is chosen to be 16 nm [8,39]. The dipole moment of a magnetic particle is proportional to its magnetic core volume with the relation of $m_i = \mu_0\pi\sigma_i^3 M_d/6$, where M_d is the bulk magnetization of the magnetic material. M_d is 4.46×10^5 A/m for magnetite, thus the dipolar coupling constant λ_0 $(=m_0^2/4\pi\mu_0 kT\sigma_0^3)$, which relates the dipole-dipole interaction energy of two contacting particles to the thermal energy kT, equals 1.3 for the small particles at room temperature $T=300$ K, and we find a value of $\lambda_L=5.32$ for the large ones. From our previous investigations [23,50] of monodisperse ferrofluids we know that a ferrofluid with $\lambda=1.3$ can be to a very good approximation described by the theoretical models, whereas a fluid with $\lambda_L=5.32$ shows significant deviations due to chain formation.

Two different cases were investigated. In the first case, we fixed the total volume fraction of the particles $\phi = \Sigma_{i=1}^{N} \pi\sigma_i^3/6V$ where V is the volume of the simulation cell. By varying the volume fraction of the large particles ϕ_L, the influence of different content of large particles on the structure and magnetic properties of ferrofluids is studied. In the second case, we fixed the volume fraction of the large particles ϕ_L and added different fractions of small particles by varying ϕ_S in order to study the effect of the presence of small particles on the aggregation behavior of the large ones [41,42].

A. Constant total volume fraction of particles

In this part the total volume fraction of the particles is fixed to an experimentally relevant value of $\phi=0.07$ [8]. The fraction of the large particles is varied from $\phi_L=0$ to 0.07, so that we go from the monodisperse system consisting of small particles through the bidisperse cases, and finally to the monodisperse system of large particles. The samples with variable content of large particles can be experimentally obtained at various stages of the magnetic purification process [8]. The total number N of particles in the simulation box was mainly taken to be $N=1000$. But a much larger number of N $(=3029)$ was also employed in the case of $\phi_L=0.007$ in order to get good statistics with a sufficient number of large particles. This specific value of ϕ_L was used in a theoretical model to describe the observed magnetoviscous effects of a commercial ferrofluid (APG513A) by a bidisperse model [8,39].

1. Magnetic properties

The magnetic properties of polydisperse ferrofluid systems have been the subject of several theoretical works [34–37,25,53]. When the particle concentration is sufficiently low, the ferrofluid system behaves like an ideal paramagnetic gas. Its physical properties are well described by the one-particle model [34]. The equilibrium magnetization of such a system can be written in terms of the Langevin function $\mathcal{L}(\alpha)=\coth(\alpha)-1/\alpha$,

$$M_L(H)=\sum_{i=1}^{N} m_i \mathcal{L}(\alpha_i)/\mu_0 V, \tag{7}$$

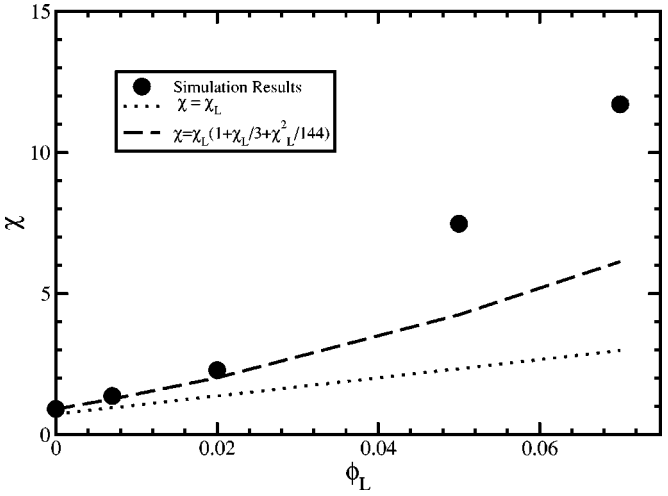

FIG. 1. Initial susceptibility as a function of the volume fraction of the large particles, together with the theoretical predictions of Eqs. (8) and (9). The total volume fraction of particles is fixed to $\phi=0.07$.

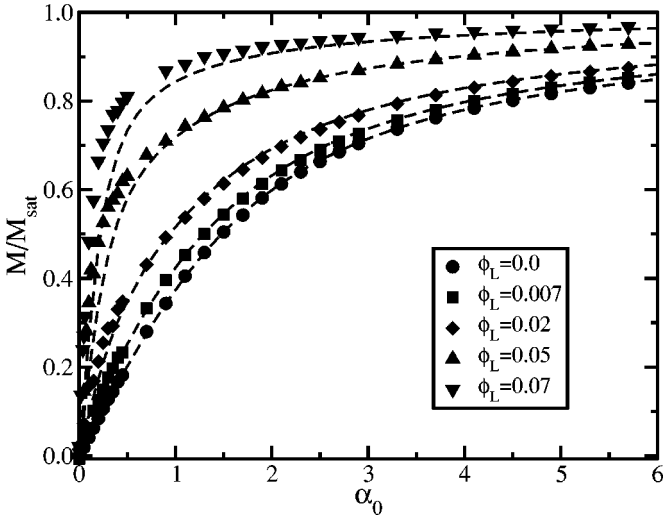

FIG. 2. Magnetization curves of the systems with different volume fraction of large particles ϕ_L. The dimensionless Langevin parameter $\alpha_0(=m_0H/kT)$ is used to denote the field strength. The total volume fraction of particles is fixed to $\phi=0.07$. The theoretical results (dashed curves) are obtained from Eq. (10).

where $\alpha_i=m_iH/kT$ is the Langevin parameter and H is the internal field. Equation (7) predicts a Curie's law for the initial susceptibility that depends linearly on the particle concentration

$$\chi_L=n\langle m^2\rangle/3\mu_0kT=\sum_{i=1}^{N} m_i^2/3\mu_0kTV, \tag{8}$$

where $n=N/V$ is the number density of the particles. It can also be written as $\chi_L=8(\phi_S\lambda_0+\phi_L\lambda_L)$ in the bidisperse systems. When ϕ or the dipolar coupling is increased, the interparticle interactions must be taken into account. A prediction for the initial susceptibility χ up to cubic accuracy in χ_L was obtained as [36,53,54]

$$\chi=\chi_L(1+\chi_L/3+\chi_L^2/144). \tag{9}$$

The corresponding formula for the magnetization M was given by the modified mean-field model [32,36]

$$M(H)=M_L(H_e), \tag{10}$$

with the effective field acting on an individual magnetic particle

$$H_e=H+\frac{M_L(H)}{3}+\frac{1}{144}M_L(H)\frac{dM_L(H)}{dH}. \tag{11}$$

The initial susceptibility χ is determined by the linear magnetic response $\mathbf{M}=\chi\mathbf{H}$ at field strength $H\to 0$. In our simulations the values of χ were obtained by calculating the equilibrium magnetization $\mathbf{M}$ for a series of weak fields $\mathbf{H}$ starting from 0 and then performing a linear fit to the $M(H)$ curves [23,50]. The results of χ are shown in Fig. 1 as a function of the volume fraction of the large particles, together with the theoretical predictions of Eqs. (8) and (9), respectively. The error bars are within the size of the symbols. As expected from the monodisperse simulations [23,50], the Langevin model [Eq. (8)] underestimates the initial susceptibility already at this moderate particle concentration. The third order prediction [Eq. (9)] describes the simulation results well at low values of ϕ_L, but deviations occur when $\phi_L\geqslant 0.02$. This discrepancy can be attributed directly to the aggregation of the large particles which is not sufficiently taken into account by the theoretical calculations [23].

The simulation results on the full magnetization curves are shown in Fig. 2, together with the theoretical predictions of Eq. (10). The dimensionless Langevin parameter α_0 $(=m_0H/kT)$ is used to denote the field strength. Since the total volume fraction of the particles is fixed, the saturation magnetization $M_{sat}(=\Sigma_{i=1}^{N}m_i/\mu_0V)$ is the same for all these systems. Under the same field strength α_0 or H, the large particles experience a higher energy mH than the small ones. Thus they are more easily oriented along the field direction. As indicated by Eqs. (7) and (10), even a small number of large particles can enhance the magnetization at weak fields significantly. This can be seen in Fig. 2 from the difference between the magnetization curves of the monodisperse system of small particles and the bidisperse system with $\phi_L=0.007$. The experimental measurements of Odenbach (Fig. 4.21 in Ref. [8]) have revealed a similar increment of M/M_{sat} with ϕ_L, where ϕ_L was systematically varied from 9×10^{-4} to 0.008 for the fixed total volume fraction of $\phi=0.07$. The good agreement between the simulation and theoretical results in this range of ϕ_L reflects that the third order theory of Eqs. (9) and (10) provides a good description of the magnetization properties of real ferrofluid systems. When we increased ϕ_L to 0.02 in our simulations, the calculated results start to rise faster at weak fields than predicted by theory. This discrepancy increases with the increase of ϕ_L. It consequently results in higher values of the initial susceptibility as shown in Fig. 1. The reason is not only related to the increased amount of large particles, but more

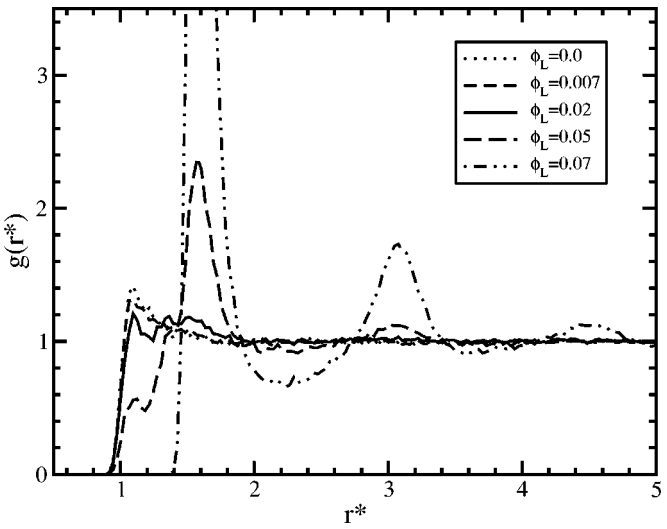

FIG. 3. Radial distribution function of the systems with different volume fraction of large particles ϕ_L at zero field. The total volume fraction of particles is fixed to $\phi=0.07$.

importantly to the aggregation of them, as has already been seen in the monodisperse case [23]. When the field strength is high enough, the dipole moments of all particles are forced to align along the field direction. The influence of the clusters becomes negligible. This is the reason why the simulation results agree with the theoretical predictions very well for all systems at high values of α_0.

2. Structure formation

Figure 3 gives the radial distribution function (RDF) of different systems at zero field. The RDF of the monodisperse system of small particles is nearly the same as that of a hard-sphere system with diameter $\sigma^*=1$. It reflects that the particles remain homogeneously distributed, because the dipole-dipole interaction energy is comparable with thermal energy in this case. The result for $\phi_L=0.007$ only slightly differs from that of the monodisperse small particle system. The molar fraction of the large particles ($N_L/N=2.6\%$) is still too small to affect the global structure of the RDF. The simulation results on the magnetic properties agree with the theoretical predictions very well in this case. When ϕ_L is increased to 0.02, two small peaks appear at around $r^* \approx 1.3$ and 1.6 in addition to the one at $r^* \approx 1$, as expected for a binary mixture of hard spheres with diameters $\sigma^*=1.0$ and 1.6. These peaks reflect the possibility of some dimer and trimer formations in the system. The aggregation behavior becomes evident when $\phi_L=0.05$. The sharpness of the peak at $r^* \approx 1.6$ and the appearance of the peak at $r^* \approx 3.1$ indicate the formation of clusters or short chains by the large particles. There is no apparent evidence, such as the sharpness of the peak at $r^*=1.3$, to show the high probability of small particles aggregating with the large ones in this case. When the system consists of only large particles, the very sharp first peak [$g(1.6) \approx 8.4$] as well as the following second and third peaks reflect the formation of long chains in the system. The discrepancy between the simulation and theoretical results on χ and $M(H)$ at higher values of ϕ_L is apparently due to the aggregation of the large particles. The structure character of these systems can be seen from the snapshots of the three-dimensional configurations in Fig. 4. Since the small particles are mainly in a nonaggregating state, only the large particles are shown there. For a quantitative understanding we have carried out a detailed cluster analysis to characterize the structures formed in different systems.

The cluster analysis of the ferrofluid systems is based on an energy criterion. Two particles are considered to be bound if their dipolar interaction energy is less than a predefined value $U_{bond}=-1.4\lambda_0 kT[2\sigma_i^*\sigma_j^*/(\sigma_i^*+\sigma_j^*)]^3$, or 70% of the contact energy of two perfectly coaligned dipolar particles [13,17,19,23,28]. The average cluster size is defined by

$$S_{avg}=\left\langle \sum_s sn_s \Big/ \sum_s n_s \right\rangle, \tag{12}$$

where n_s is the number of clusters having size s, and the angular brackets denote the time average, or equivalently, the average over the configuration space. In the monodisperse system of small particles, the average cluster size is slightly above 1 at zero field and increases weakly with the field strength [23]. This is consistent with the result in Fig. 3 that reflect the nonaggregating behavior of the small particles. Thus our cluster analysis was mainly focused on the structures formed by the large particles. The results on large particles are distinguished by adding a subscript L to the parameters in Eq. (12).

Figure 5 shows the average cluster size $S_{avg,L}$ in case of zero field as a function of ϕ_L. The increase of $S_{avg,L}$ indicates that the large particles form longer chains with the increase of their volume fraction. This can be more clearly demonstrated by calculating the time average value of $\langle s_L n_{s,L}\rangle/N_L$ which means the average fraction of large particles in clusters of size s_L, or in other word, the probability of finding a large particle in a cluster of size s_L. The results obtained at the zero field are given in Fig. 6.

The dotted curve in Fig. 6 shows that in case of $\phi_L=0.007$ about 65% of the large particles remain in the nonaggregated individual state. The others aggregate into short clusters as dimers and trimers. As a result, the average cluster size is about $S_{avg,L}=1.23$. The simulations using total number of particles $N=1000$ and 3029 provide consistent results within the error bars. This value of $S_{avg,L}$ is apparently smaller that predicted in Ref. [39] (about 2.7) for a bidisperse system with parameters very close to ours. This discrepancy may be related to the strong assumptions employed in the theoretical calculations, e.g., neglecting the interactions between the large particles with the surrounding small ones and describing the chain formation as a process proceeding in a magnetically neutral medium. However, the presence of the small particles strongly affects the aggregation behavior of the large ones. This can be elucidated by a qualitative discussion. Since the density of the large particles is relatively small, the average separation between them is several times larger than the diameter of the small ones. The large amount of small particles construct a magnetic background for the large ones. If the large-small particle interactions can be ne-

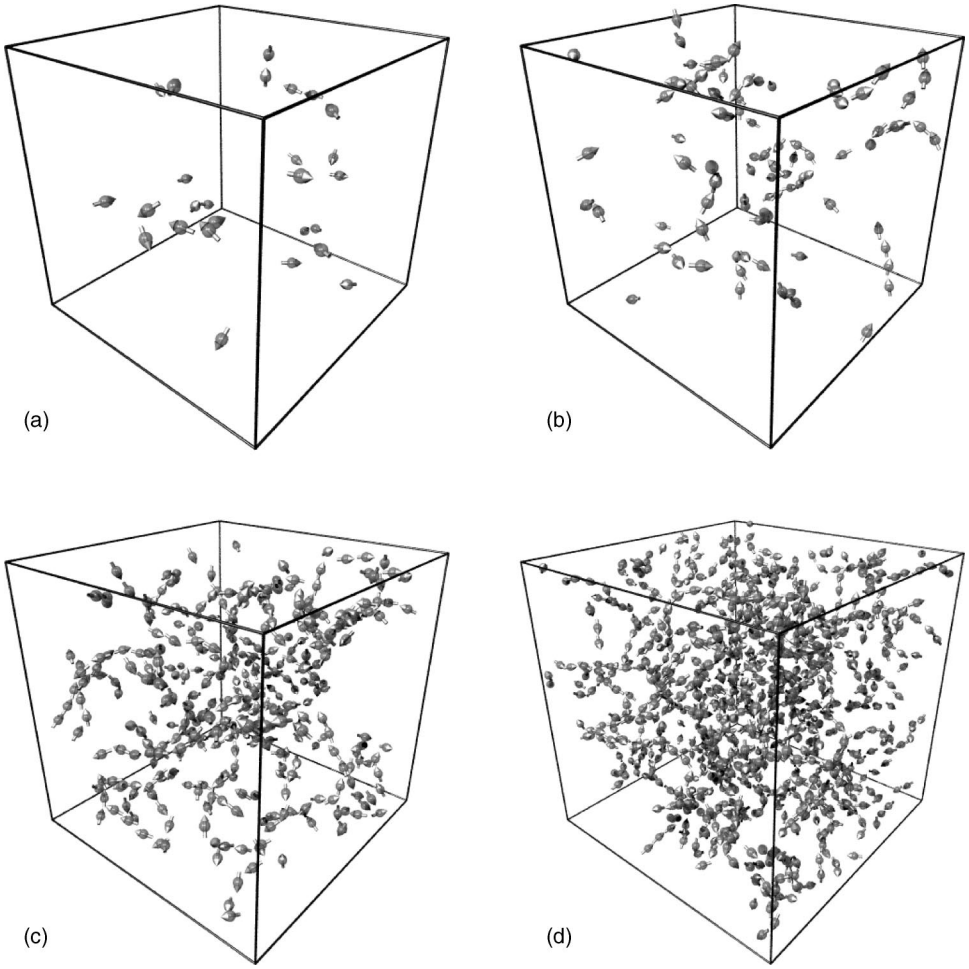

FIG. 4. Snapshots of the structures formed in different systems at zero field. The total volume fraction of particles is fixed to $\phi=0.07$ in all cases. The total number of particles is $N=1000$, but only the large particles are shown here. The volume fraction of the large particles ϕ_L is varied as (a) 0.007, (b) 0.02, (c) 0.05, and (d) 0.07. Correspondingly, the side length of the cubic simulation box L^* is varied as (a) 20.07, (b) 21.19, (c) 25.33, and (d) 31.29, respectively. The arrows with length σ_L^* indicate the orientation of the dipole moments. The spheres with diameter of $\sigma_L^*/2$ give the center positions of the particles.

glected, this background could be assumed as a continuous magnetic medium. For the present case of $\phi_L=0.007$, the magnetic permeability μ_{eff} of this medium is about 1.8 given by Eq. (9) and our simulations, considering the condition of $\phi_S=0.063$ and $\lambda_0=1.3$. The dipolar interaction energy between two large particles in such a magnetic medium is in average μ_{eff} times smaller than that in a neutral medium. This weakening of the interaction energy will effectively reduce the aggregation probability of the large particles. Although the thermal fluctuations still allow these particles to approach each other to form short clusters, the further aggregation is again inhibited by the accompanying increase of the

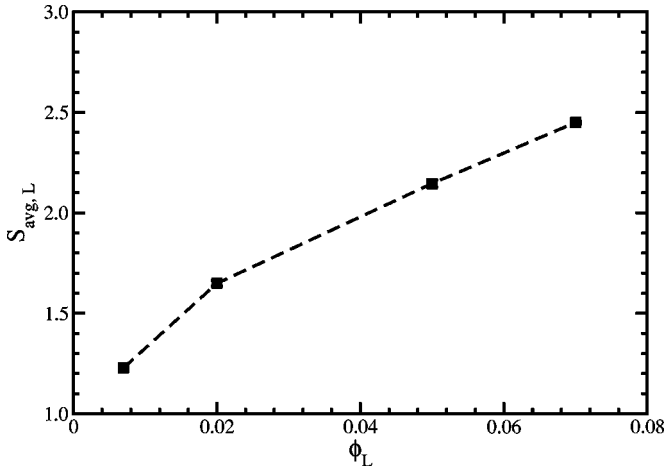

FIG. 5. Average size of clusters formed by large particles at zero field as a function of the volume fraction of the large particles ϕ_L. The total volume fraction of particles is fixed to $\phi=0.07$.

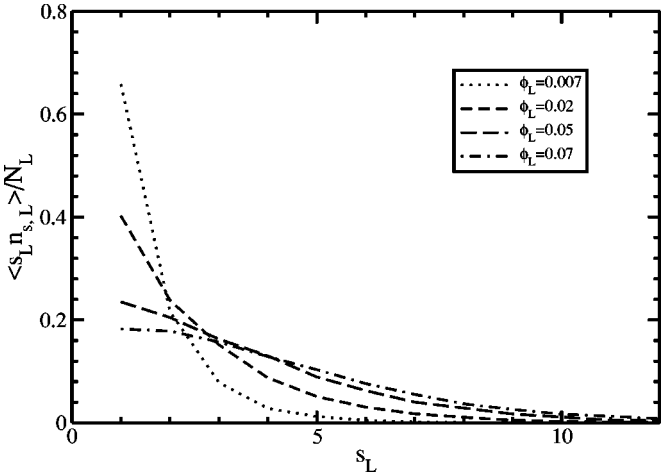

FIG. 6. Average fraction of large particles which take part in forming the clusters of size s_L at zero field. The total volume fraction of particles is fixed to $\phi=0.07$.

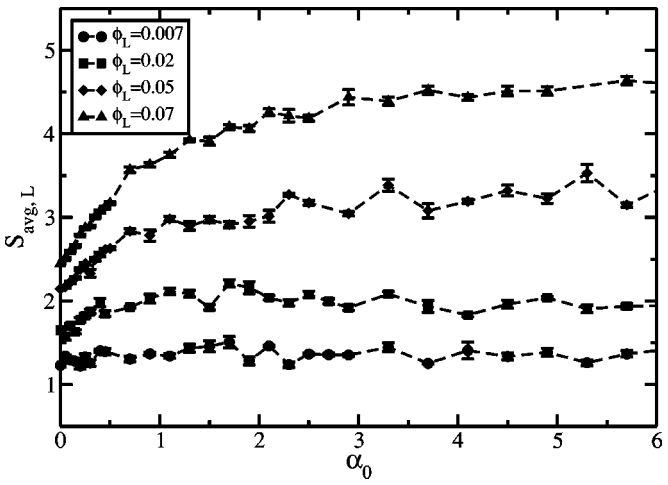

FIG. 7. Field dependence of the average size of clusters formed by the large particles. The total volume fraction of particles is fixed to ϕ=0.07.

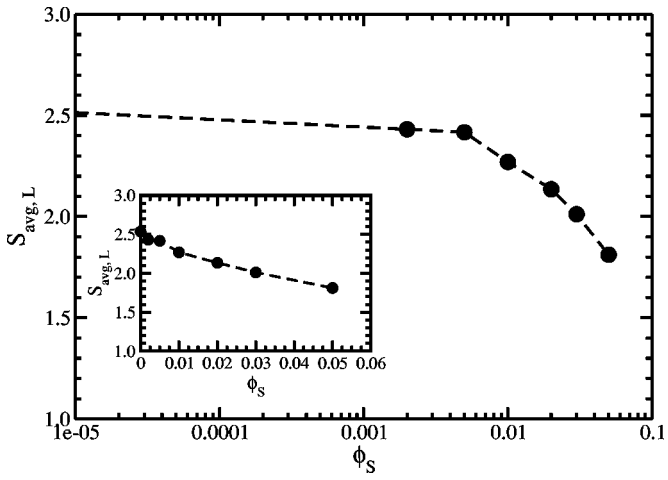

FIG. 8. Average size of clusters formed by the large particles as a function of the volume fraction of the small particles ϕ_S. The volume fraction of the large particles is fixed to $\phi_L = 0.05$.

average separation between them. Thus, neglecting the presence of small particles will lead to an overestimating of the average cluster size formed by large particles. The above discussion is a primary approximation more valid in the limit of $\phi_L/\phi_S \ll 1$ and $\sigma_S/\sigma_L \ll 1$. Considering that both the dipole-dipole and short-range interactions between the large and small particles are included in the simulations, our simulation result on $S_{avg,L}$ is reasonably smaller than that predicted in the theoretical calculations. If the diameter of the small particles in our simulations is taken to be a smaller value, for example 7.8 nm, the difference between the simulation and theoretical results might be reduced.

When ϕ_L is increased, the clusters grow in both size and number. The distribution of $\langle s_L n_{s,L} \rangle / N_L$ turns to be more flat and broad. There is a crossover of these distribution curves at $s_L \approx 3$, reflecting that more and more individual particles or short clusters are aggregating into longer chains with the increase of ϕ_L. In the monodisperse system of large particles, the most probable chain length for finding a particle is shifted from monomer to dimer, as indicated by the plateau at $s_L \approx 2$. Correspondingly, the average cluster size $S_{avg,L}$ is increased to about 2.45 in this case. The system with $\phi_L = 0.05$ provides a situation where the molar fractions of the large and small particles are comparable. The effect of the small particles as a magnetic background is weaker, they influence the aggregation behavior of the large ones more in a perturbative way, as will be discussed in the following section.

The application of an external field can enhance the aggregation of the large particles, since it forces the dipole moments and the chainlike clusters to align along the field direction, and thus increases the probability for them to combine with each other in a head-to-tail way. The field dependence of the average cluster size is shown in Fig. 7. It can be seen that, in general, the value of $S_{avg,L}$ increases with the field strength in the weak field regime, and gradually saturates at strong field strength. However, the total increment of the average cluster size is insignificant in case of small ϕ_L. The saturation value of $S_{avg,L}$ is reached at relatively low field strength. For $\phi_L = 0.007$ this value is only about 10% higher than that at zero field. Since the aggregation of the large particles in this case might be slowed down due to their large separation and the presence of small particles, we have carried out some long simulation runs (dimensionless time $t^* = 1600$) with $N = 3029$ in order to make sure that we obtain truly equilibrium results for this case. The effect of the magnetic field becomes evident when $\phi_L \geqslant 0.02$, where the simulation results on the magnetic properties start to deviate from the theoretical predictions. The increment amplitude of $S_{avg,L}$ rises rapidly with the increase of ϕ_L. When $\phi_L = 0.07$, the saturation value of $S_{avg,L}(\approx 4.7)$ is about twice as much as that at zero field. Most of the particles are engaged in the formation of long chain structures. The dynamics of the system turns out to be very slow due to the entanglement of the long chains. A relaxation time of $t^* \geqslant 500$ is needed to reach the equilibrium state at weak fields. Following that the values of M and $S_{avg,L}$ are calculated by averaging over a long enough simulation time ($t^* \geqslant 1000$). Since the effective viscosity of ferrofluids is mainly determined by the aggregates formed by large particles [8,39], the results in Fig. 7 suggest that strong magnetoviscous effects can be achieved from experimental samples with high fraction of large particles.

B. Constant volume fraction of large particles

In this part the volume fraction of the large particles is fixed to $\phi_L = 0.05$ where the formation of relatively long chains is expected from the monodisperse case. The number of the large particles is taken to be $N_L = 500$. The small particles are added into the system by varying their volume fraction from $\phi_S = 0$ to 0.05. The total number of the particles is accordingly increased from $N = 500$ to 2548. The influence of the small particles on the aggregation behavior of the large ones is investigated by doing cluster analysis of the structures formed in different cases.

The simulation result on the average cluster size $S_{avg,L}$ at zero field is shown in Fig. 8 as a function of ϕ_S. The same

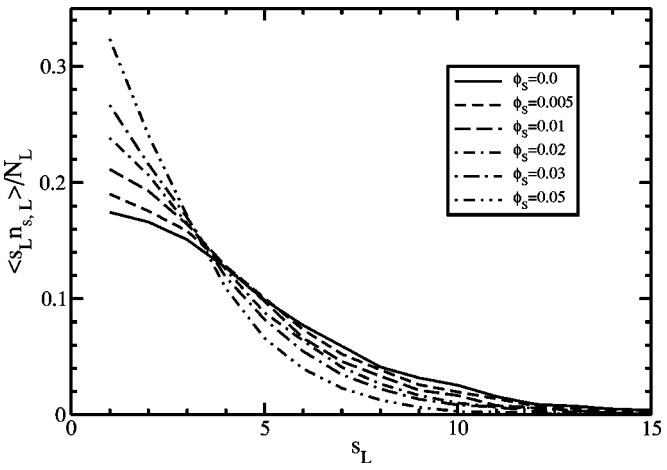

FIG. 9. Average fraction of large particles which take part in forming clusters of size s_L at zero field. The volume fraction of the large particles is fixed to $\phi_L = 0.05$.

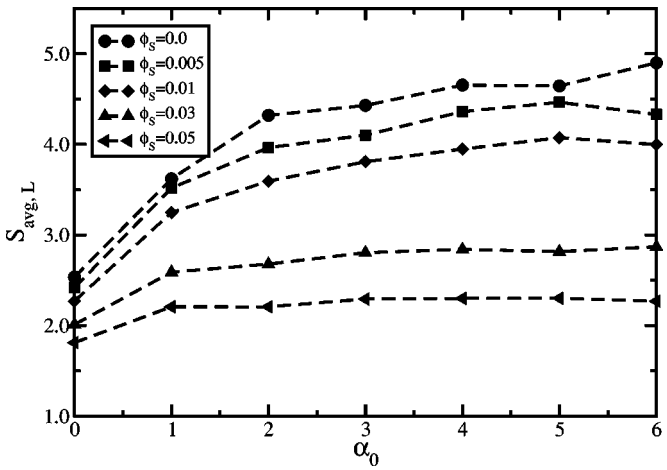

FIG. 11. Field dependence of the average size of clusters formed by the large particles.

results are plotted in two different ways by using both a linear and a logarithmic scale for the x axis. A small volume fraction ϕ_S influences only weakly the aggregation behavior of the large ones. $S_{avg,L}$ decreases slightly for $\phi_S \leqslant 0.005$. But this value drops quickly when the molar fraction of the small particles becomes comparable or higher than that of the large ones. The variation of the distribution $\langle s_L n_{s,L} \rangle / N_L$ is shown in Fig. 9 for different systems at zero field. The crossover of these data curves occurs in between $s_L = 3$ and 4. The value of $\langle s_L n_{s,L} \rangle / N_L$ increases with ϕ_S before the crossover point, but decreases after that. It reflects that the long chain structures are broken into small segments like monomers, dimers, or trimers due to the addition of the small particles. The breaking of the chain structures is also reflected by the observed decrease of the height of the peaks at $r^* \approx 1.6$ and 3.1 in the RDF of these systems, see Fig. 10.

Figure 11 presents the field dependence of $S_{avg,L}$ for the systems with different ϕ_S. The increment amplitude of $S_{avg,L}$ with the field strength decreases with the increasing fraction of small particles, similar to that in Fig. 7 although ϕ_L is fixed here. The ratio between the saturation and zero-field values of $S_{avg,L}$ drops from about 1.84 in the monodisperse case to about 1.28 at $\phi_S = 0.05$. The field dependence of the cluster size distribution can be seen in Fig. 12 where the results of $\langle s_L n_{s,L} \rangle / N_L$ are plotted for the case of $\phi_S = 0.01$. In this case the molar fractions of the small and large particles are comparable. The most probable chain length for finding a large particle appears at $s_L = 3$ for $\alpha_0 = 1$, and then shifts to larger values with increased α_0. The distribution curve gradually saturates after $\alpha_0 \geqslant 3.0$. The results obtained for other values of ϕ_S present a similar behavior. They differ in that at same α_0 the distribution curve turns to be more flat and broad with decreasing ϕ_S, and accordingly the most probable chain length also shifts to larger s_L. The above results strongly suggest that the presence of the small particles could not be neglected for discussing the structuring behavior of large particles in bidisperse ferrofluid systems.

Since ϕ_L is fixed to 0.05, the mean separation between the surfaces of the large particles is about $2.5\sigma_0$. It means that in average only two small particles are able to get in the

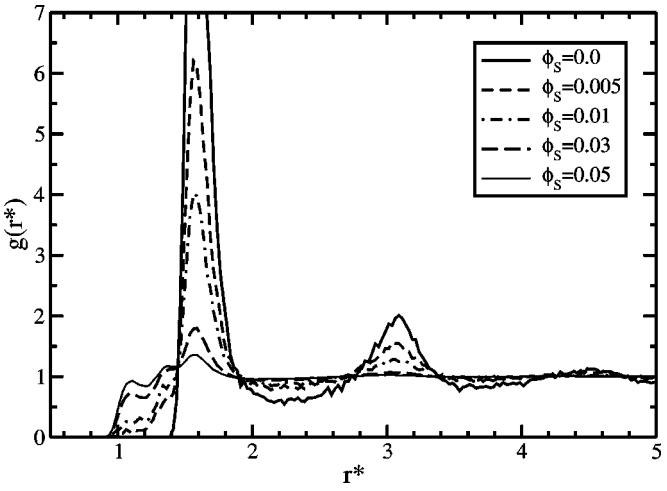

FIG. 10. Radial distribution functions of the systems with different volume fraction of small particles ϕ_S at zero field. The volume fraction of the large particles is fixed to $\phi_L = 0.05$.

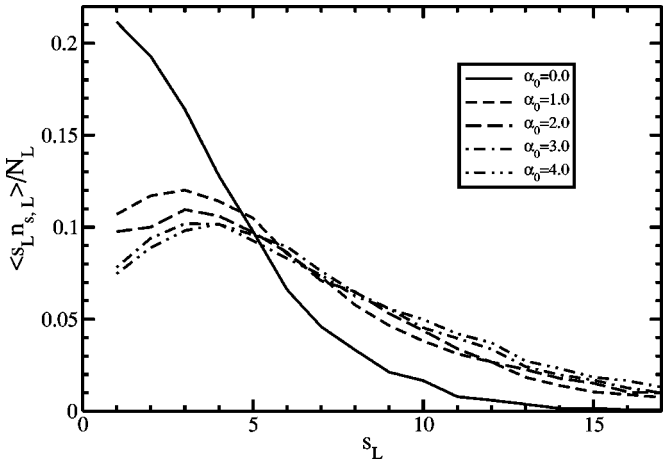

FIG. 12. Field dependence of the distribution $\langle s_L n_{s,L} \rangle / N_L$ in case of $\phi_L = 0.05$ and $\phi_S = 0.01$.

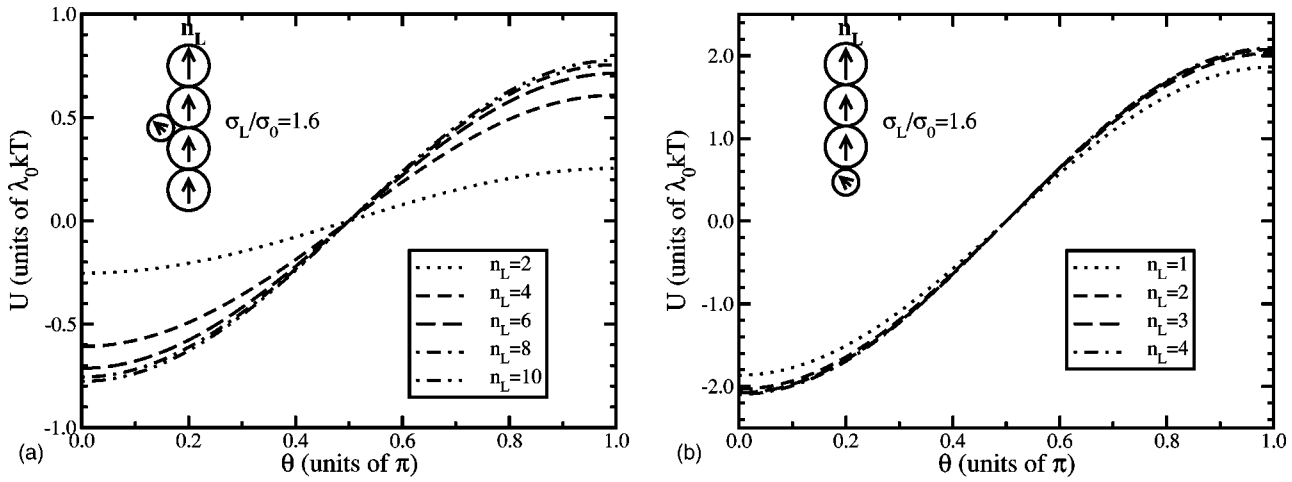

FIG. 13. Dipolar energy of a small particle when it is attached to the side (a) or end (b) of a straight chain formed by large particles with well aligned dipole moment orientations. θ is the angle between the orientation of the dipole moment of the small particle and the axis of the chain. In (a) the small one is attached to the triangular position constructed by the two large particles in the middle of the chain.

space between two large particles. This makes the system different from the case of very low ϕ_L, especially when ϕ_S is low. The small particles affect the aggregation behavior of large ones more in a perturbative way in this case. On one hand, the small particles perform Brownian motions and interact with the large ones through excluded volume interactions. These lead to fluctuations in the chain structures, rendering them more unstable. This is especially the case when the small particles are neutral spheres, as has been shown in Ref. [45]. On the other hand, the small particles may also aggregate with the chains formed by large particles due to their dipole-dipole interaction. There are two possible ways for them to be combined with these chains. One is moving from the transverse direction perpendicular to the chain axis and being trapped at the triangular position constructed by two contacting large particles. The other is being attached to the ends of the chains. The dipolar energy of a small particle in these two cases is shown in Fig. 13 as a function of the chain length s_L. The chains are assumed to be straight with all the dipole moments well coaligned. The maximum attractive energy is obtained in case of the dipole moment of the small one orienting in parallel with the chain axis. However, this energy is not stronger than kT in the transversely attaching case [Fig. 13(a)] even if the chain length is longer than 10. The small ones will always go to the ends of the chains due to the relatively strong attraction as shown in Fig. 13(b). In this case the attractive energy is not very sensitive to the chain length s_L due to the $1/r^3$ character of the dipolar potential. If the number of small particles is large, they have a relatively high probability to be attached to the ends of the chains. When two short chains with small particles at their ends approach each other and combine into a longer chain, the small ones in the middle make the long chain much more unstable compared to the chains formed only by large particles. Under thermal fluctuations, these chains may easily break at the location of the small particles. This effect finally restricts the further growth of the chains and leads to the decrease of $S_{avg,L}$ with increased ϕ_S [42].

The above argument can be clarified by studying the topological structure of the clusters. At first the energy criterion is employed to detect all clusters formed by all present particles. For all the clusters of size $s \geqslant 3$, we check whether they contain small particles. The location of these small particles can be distinguished according to the linear character of the chains: a particle with two neighbors is in the middle of the chain, while that with only one neighbor is at the end. Figure 14 shows the average number of small particles in each chain. Together with them are the average number of those small ones attached at the ends of each chain. As expected, these numbers increase with the increase of ϕ_S as well as the field strength. In all cases the probability of finding an aggregated small particle at the chain ends is higher than 90%. It reflects the instability of the chains with embedded small particles in the middle, and thus supports the

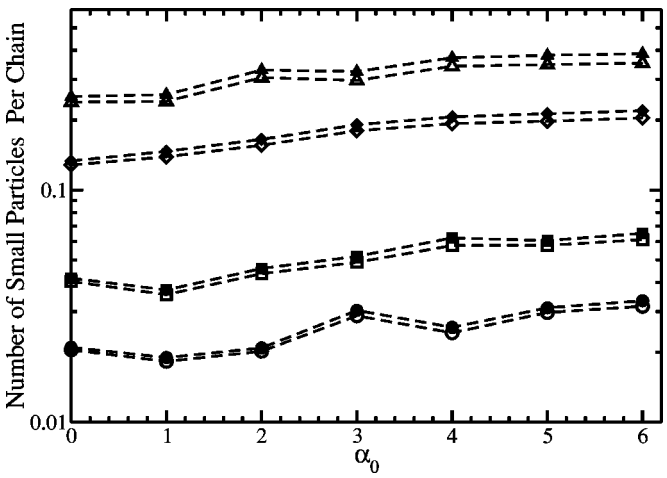

FIG. 14. Average number of small particles (solid symbols) in each chain which has length $s \geqslant 3$ as a function of dimensionless field. The open symbols correspond to the average number of small particles which are attached at the ends of each chain. ϕ_L is fixed to 0.05, and ϕ_S is taken to be 0.005 (circle), 0.01 (square), 0.03 (diamond), and 0.05 (triangle), respectively.

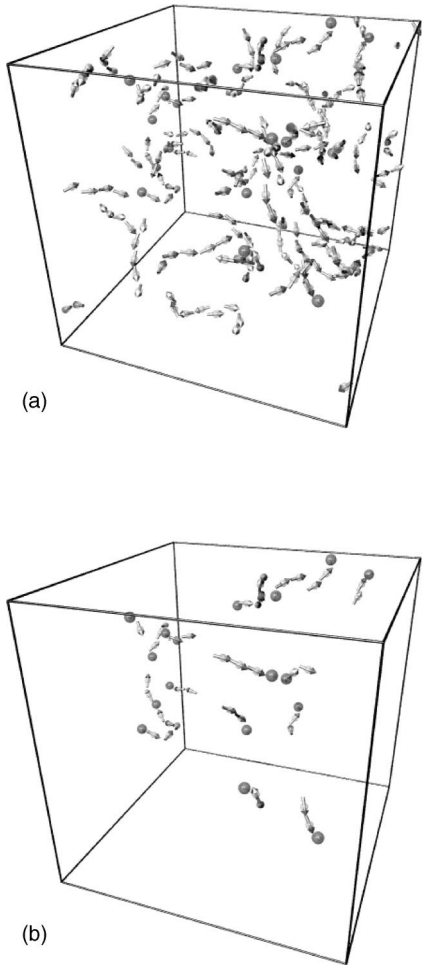

FIG. 15. Snapshot of a three-dimensional configuration formed in the system with $\phi_S = 0.05$ at zero field. (a) Only the particles aggregated into the clusters of size $s \geqslant 3$ are shown; (b) only those clusters containing small particles are shown. The side length of the simulation box is $L^* = 27.78$. The arrows with length σ_i^* indicate the orientation of the dipole moments. The small particles are shown to be darker spheres of diameter $\sigma^* = 1$, while the large particles are presented with spheres of diameter $0.4\sigma_L^*$ in order to give their center positions.

theoretical discussion of Kantorovich *et al.* [42] that the most stable structures in bidisperse ferrofluid systems are the short chains with large particles in the middle and possible one to two small ones at the ends. This can be seen clearly from the snapshot (Fig. 15) of a configuration formed in the system with $\phi_S = 0.05$ at zero field. In Fig. 15(a) only the particles aggregated into clusters of size $s \geqslant 3$ are shown. These clusters are mainly formed by large particles. There are 17 small particles combined in the 61 clusters. As shown in Fig. 15(b), where only the clusters containing small particles are plotted, almost all these small particles are attached to the ends of the short chains. The only exception is the one combined in the middle of a chain of length $s = 5$, see the left side of the simulation box in Fig. 15(b). Figure 15 and the data in Fig. 14 indicate that the average number of small particles in each chain is less than 1. The simple reason is that the binding energy between the small and large particles is not strong enough, the small particles can easily escape due to thermal fluctuation. This result can also be understood in terms of the relatively short binding time of the small particles to the chains. The use of a different value of the energy criterion U_{bond} may change the quantitative results slightly, but will not cause any qualitative difference.

The theoretically predicted phase separation or demixing of the large and small particles in bidisperse dipolar systems [43] is not observed explicitly in our simulations. The condensation of the large particles may have been prevented by the formation of chains or clusters in our systems [45,44,21], or we are still out of the regime of ϕ_S and ϕ_L where the phase separation may occur. The phase behavior of the bidisperse dipolar systems will depend on both the size ratio of the two kinds of particles, as well as on their volume fractions. A Gibbs ensemble Monte Carlo method like in Ref. [45] would probably be a better way for studying this problem.

IV. CONCLUSION

Molecular dynamics simulations have been used to calculate the equilibrium properties of bidisperse ferrofluid systems with different fractions of small and large particles, and the results are compared with theoretical predictions. In the first investigated case, the total volume fraction of particles was fixed and the volume fraction ϕ_L of the large particles was varied. The magnetic properties of the investigated systems were found to depend on the volume fraction of the large particles. When ϕ_L is small, our results on the initial susceptibility and magnetization curves agree with the third order theoretical predictions very well [36,54]. However, deviations start to appear at larger values of ϕ_L. Our detailed cluster analysis indicates that this is due to the aggregation of the large particles. The average size of the clusters formed by large particles increases with the increased ϕ_L. As a result, the magnetization of the systems at weak fields is strongly enhanced, which consequently leads to higher values of the initial susceptibility. This behavior is fully consistent with that detected for a monodisperse system at large dipolar coupling constant [23,50].

In the second case, the volume fraction of the large particles was fixed to a value where, for the monodisperse case, the particles will form relatively long chains. Small particles were added by varying their volume fraction ϕ_S. The average chain length formed by the large particles was found to decrease quickly with the increase of ϕ_S, demonstrating that the aggregation behavior of the large particles is hindered by the presence of the small particles. On a qualitative level this can be understood since a homogeneous distribution of many small particles changes the effective magnetic permeability of the background for the large particles, and thus diminishes the effective dipolar interactions between them. In addition the Brownian motion of the small particles enhances the breakup probability of longer chains. The topological analysis of the configurations in our simulations indicates that most of the chains are formed by the large particles. The number of small particles per chain is smaller than 1, and if a small particle is member of a chain, it is predominantly

attached to the end of the chain. Our findings are consistent with the theoretical discussions in Ref. [42]. Our results show that for a sufficient concentration of small particles, their presence cannot be neglected in describing the structural properties of a bidisperse ferrofluid system.

ACKNOWLEDGMENTS

We enjoyed considerable discussions with A. O. Ivanov, S. Odenbach, and A. Y. Zubarev. Financial support from the DFG under Grant No. HO 1108/8-3 is greatly appreciated.

[1] R.E. Rosensweig, *Ferrohydrodynamics* (Cambridge University Press, Cambridge, 1985).
[2] C.F. Hayes, J. Colloid Interface Sci. **52**, 239 (1975).
[3] E.A. Peterson and D.A. Krueger, J. Colloid Interface Sci. **62**, 24 (1977).
[4] H. Mamiya, I. Nakatani, and T. Furubayashi, Phys. Rev. Lett. **84**, 6106 (2000).
[5] J.C. Bacri *et al.*, J. Colloid Interface Sci. **132**, 43 (1989).
[6] S. Odenbach and H. Gilly, J. Magn. Magn. Mater. **152**, 123 (1996).
[7] S. Odenbach and H. Störk, J. Magn. Magn. Mater. **183**, 188 (1998).
[8] S. Odenbach, *Magnetoviscous Effects in Ferrofluids*, *Lecture Notes in Physics, Monographs 71* (Springer, Berlin, 2002).
[9] D. Wei and G.N. Patey, Phys. Rev. Lett. **68**, 2043 (1992).
[10] D. Wei and G.N. Patey, Phys. Rev. A **46**, 7783 (1992).
[11] J.J. Weis, D. Levesque, and G.J. Zarragoicoechea, Phys. Rev. Lett. **69**, 913 (1992).
[12] J.J. Weis and D. Levesque, Phys. Rev. E **48**, 3728 (1993).
[13] D. Levesque and J.J. Weis, Phys. Rev. E **49**, 5131 (1994).
[14] G. Ayton, M.J.P. Gingras, and G.N. Patey, Phys. Rev. Lett. **75**, 2360 (1995).
[15] B. Groh and S. Dietrich, Phys. Rev. E **50**, 3814 (1994).
[16] B. Groh and S. Dietrich, Phys. Rev. E **53**, 2509 (1996).
[17] J.J. Weis and D. Levesque, Phys. Rev. Lett. **71**, 2729 (1993).
[18] M.A. Osipov, P.I.C. Teixeira, and M.M. Telo da Gama, Phys. Rev. E **54**, 2597 (1996).
[19] J.M. Tavares, J.J. Weis, and M.M. Telo da Gama, Phys. Rev. E **59**, 4388 (1999).
[20] P.J. Camp and G.N. Patey, Phys. Rev. E **62**, 5403 (2000).
[21] A.Y. Zubarev and L.Y. Iskakova, Phys. Rev. E **65**, 061406 (2002).
[22] L.Y. Iskakova and A.Y. Zubarev, Phys. Rev. E **66**, 041405 (2002).
[23] Z. Wang, C. Holm, and H.W. Müller, Phys. Rev. E **66**, 021405 (2002).
[24] K.I. Morozov, A.F. Pshenichnikov, Y.L. Raikher, and M.I. Shliomis, J. Magn. Magn. Mater. **65**, 269 (1987).
[25] Y.A. Buyevich and A.O. Ivanov, Physica A **190**, 276 (1992).
[26] M.E. van Leeuwen and B. Smit, Phys. Rev. Lett. **71**, 3991 (1993).
[27] M.J. Stevens and G.S. Grest, Phys. Rev. Lett. **72**, 3686 (1994).
[28] M.J. Stevens and G.S. Grest, Phys. Rev. E **51**, 5962 (1995).
[29] M.J. Stevens and G.S. Grest, Phys. Rev. E **51**, 5976 (1995).
[30] A.Y. Zubarev and A.O. Ivanov, Phys. Rev. E **55**, 7192 (1997).
[31] P.J. Camp, J.C. Shelley, and G.N. Patey, Phys. Rev. Lett. **84**, 115 (2000).
[32] A.F. Pshenichnikov, V.V. Mekhonoshin, and A.V. Lebedev, J. Magn. Magn. Mater. **161**, 94 (1996).
[33] B.M. Lacava *et al.*, Appl. Phys. Lett. **77**, 1876 (2000).
[34] M.I. Shliomis, Usp. Fiz. Nauk **112**, 437 (1974) [Sov. Phys. Usp. **17**, 153 (1974)].
[35] K.I. Morozov and A.V. Lebedev, J. Magn. Magn. Mater. **85**, 51 (1990).
[36] A.O. Ivanov and O.B. Kuznetsova, Phys. Rev. E **64**, 041405 (2001).
[37] B. Huke and M. Lücke, Phys. Rev. E **67**, 051403 (2003).
[38] J.C. Bacri, R. Perzynski, and D. Salin, J. Magn. Magn. Mater. **85**, 27 (1990).
[39] A.Y. Zubarev, J. Exp. Theor. Phys. **120**, 80 (2001).
[40] S.M.A. Bradbury and R.W. Chantrell, J. Magn. Magn. Mater. **54-57**, 745 (1986).
[41] S. Kantorovich and A.O. Ivanov, J. Magn. Magn. Mater. **252**, 244 (2002).
[42] S. Kantorovich, J. Magn. Magn. Mater. **258-259**, 471 (2003).
[43] A.O. Ivanov, J. Magn. Magn. Mater. **154**, 66 (1996).
[44] B.J.C. Cabral, J. Chem. Phys. **112**, 4351 (2000).
[45] M.J. Blair and G.N. Patey, Phys. Rev. E **57**, 5682 (1998).
[46] X.S. Chen, M. Kasch, and F. Forstmann, Phys. Rev. Lett. **67**, 2674 (1991).
[47] S.W. de Leeuw, J.W. Perram, and E.R. Smith, Proc. R. Soc. London, Ser. A **373**, 27 (1980).
[48] M.P. Allen and D.J. Tildesley, *Computer Simulation of Liquids*, 1st ed. (Clarendon Press, Oxford, 1987).
[49] Z. Wang and C. Holm, J. Chem. Phys. **115**, 6351 (2001).
[50] Z. Wang, C. Holm, and H.W. Müller, J. Chem. Phys. **119**, 379 (2003).
[51] V.V. Murashov and G.N. Patey, J. Chem. Phys. **112**, 9828 (2000).
[52] P.G. Kusalik, J. Chem. Phys. **93**, 3520 (1990).
[53] M.S. Wertheim, J. Chem. Phys. **55**, 4291 (1971).
[54] B. Huke and M. Lücke, Phys. Rev. E **62**, 6875 (2000).